Poultry Science

Osteocalcin activates lipophagy via the ADPN-AMPK/PPARα-mTOR signaling pathway in chicken embryonic hepatocyte

W. J. Tu,* Y. H. Zhang,* X. T. Wang,* M. Zhang,† K. Y. Jiang,* and S. Jiang *,[1]

*Joint International Research Laboratory of Animal Health and Animal Food Safety, College of Veterinary Medicine, Southwest University, Chongqing 400715, China; and †Sichuan Sanhe College of Professionals, Sichuan, China

ABSTRACT Fatty liver hemorrhage syndrome (**FLHS**) is the leading cause of noninfectious mortality in caged layers worldwide. Osteocalcin (**OCN**) is a protein secreted by osteoblasts, and its undercarboxylated form (**ucOCN**) acts as a multifunctional hormone that protects laying hens from FLHS. Lipophagy is a form of selective autophagy that breaks down lipid droplets (**LDs**) through lysosomes, and defective lipophagy is associated with FLHS. The aim of this study was to investigate the effects of ucOCN on the lipophagy of chicken embryonic hepatocytes and associated the function of the adiponectin (**ADPN**) signaling pathway. In this study, chicken embryonic hepatocytes were divided into 5 groups: control (**CONT**), fat emulsion (**FE**, 10% FE, v/v), FE with ucOCN at 1 ng/mL (**FE-LOCN**), 3 ng/mL (**FE-MOCN**), and 9 ng/mL (**FE-HOCN**). In addition, 4 μM AdipoRon, an adiponectin receptor agonist, was used to investigate the function of ADPN. The results showed that compared with CONT group, FE promoted the levels of phosphorylation of mammalian target of rapamycin (**p-mTOR**) ($P < 0.05$) and decreased the mRNA expression of ADNP receptors (*AdipoR1* and *AdipoR2*). Compared with FE group, 3 and 9 ng/mL ucOCN inhibited the levels of autophagy adaptor p62 and p-mTOR ($P < 0.05$), increased the ratios of LC3-II/LC3-I ($P < 0.05$) and phosphorylated adenosine 5′-monophosphate-activated protein kinase (**p-AMPK**)/AMPK ($P < 0.05$), as well as the levels of peroxisome proliferator-activated receptor α (**PPAR-α**) and ADPN ($P < 0.05$). In addition, ucOCN at the tested concentrations increased the colocalization of LC3 and LDs in fatty hepatocytes. Administrated 4 μM AdipoRon activated *AdipoR1* and *AidpoR2* mRNA expression ($P < 0.05$), decreased the concentrations of triglyceride ($P < 0.05$), without effects on cell viability ($P > 0.05$). AdipoRon also increased the LC3-II/LC3-I ratio ($P < 0.05$) and the levels of p-AMPK/AMPK and PPAR-α ($P < 0.05$). In conclusion, the results reveal that ucOCN regulates lipid metabolism by activating lipophagy via the ADPN-AMPK/PPARα-mTOR signaling pathway in chicken embryonic hepatocytes. The results may provide new insights for controlling FLHS in laying hens.

Key words: osteocalcin, fatty liver hemorrhagic syndrome, chicken embryonic hepatocyte, ADPN/AMPK/mTOR, lipophagy

2024 Poultry Science 103:103293
https://doi.org/10.1016/j.psj.2023.103293

INTRODUCTION

Fatty liver hemorrhage syndrome (**FLHS**) is a noninfectious metabolic disease that mainly occurs in caged layers (Rozenboim et al., 2016; Zhuang et al., 2019). FLHS in chicken is characterized by increased lipid accumulation, liver steatosis, and sudden death, consequently reduced egg production, leading to huge economic losses to the poultry egg industry (Shini et al., 2018). The accumulation of fatty acid, triglyceride (**TG**), and lipid droplets (**LDs**) in hepatocytes is the initial crucial step of FLHS, as that lipid accumulation in the liver cells triggers a number of reactions, including oxidative stress and inflammation, causing hepatocyte dysfunction (Bessone et al., 2019; Zhang et al., 2022b). Therefore, ameliorating fat built up in the liver can efficiently prevent FLHS (Lin et al., 2021; Miao et al., 2021).

Autophagy (self-cleaning), an evolutionarily conserved process, is an intracellular degradation system used for degrading and recycling various cellular components, for example, the endoplasmic reticulum (**ER**, i.e., rough ER and smooth ER) to synthesize and deliver proteins, lipids, and chondriosome for forming vacuoles and lysosomes in eukaryotic cells (Wang et al., 2020a). The

Received October 6, 2023.
Accepted November 13, 2023.

[1]Corresponding author: jiangsha0527@swu.edu.cn

degradation of LDs via autophagy has been referred to as lipophagy (Khawar et al., 2019). The LDs are conserved cellular organelles containing neutral fats such as TG, cholesterol ester, and monolayer phospholipids as well as a large number of lipoproteins (Khawar et al., 2019). Normally, free fatty acids (**FFAs**) are esterified into TG and stored in LDs to protect cells from cytotoxic effects of FFAs (Scorletti and Carr, 2022). However, excessive accumulated FFAs can cause an overload of intracellular LDs, consequently, LDs broken down and released FFAs into cytoplasm via lipolysis which is facilitated by cytosolic neutral TG lipases and autophagy (Xu and Fan, 2022). In hens with FLHS, lipophagy appears to fail, and impaired autophagy seems to be a vital factor in the progression of FLHS (Wang et al., 2020a; Wu et al., 2021). Activating autophagy, particularly lipophagy, may be an efficient strategy to ameliorate chicken FLHS.

Undercarboxylated osteocalcin (**ucOCN**) is a vitamin K-dependent noncollagenous protein synthesized by osteoblasts and has a role in regulating energy metabolism (Tacey et al., 2021). Previous studies have demonstrated that ucOCN can effectively mitigate fat emulsion (**FE**)-induced chicken embryonic hepatocyte damage, reduce LDs quantity, suppress mitochondrial disorder, decrease reactive oxygen species (**ROS**) synthesis, alleviate fat accumulation, inhibit inflammatory cytokine production and prevent apoptosis (Zhang et al., 2022a). It has also been found that ucOCN reduces insulin resistance and oxidation stress in aged laying hens fed high-fat diet (**HFD**) (Wu et al., 2021). In addition, ucOCN has function in alleviating HFD-induced inhibition of autophagy in laying hens (Wu et al., 2021). However, the effect of ucOCN on autophagy of liver cells needs to be further investigated or studied.

Adiponectin (**ADPN**) is a hormone secreted by adipose tissue, with 2 receptors named as AdipoR1 and AdipoR2 (Gamberi et al., 2018). These 2 receptors activate the AMP-activated protein kinase (**AMPK**) and Peroxisome proliferator-activated receptor alpha (**PPAR*α***) signaling pathways, respectively (Cao et al., 2022). The AMPK functions as an energy sensor, playing an important role in autophagy, metabolic homeostasis, and lipid deposition (Yao et al., 2022a). The PPARα is a regulator of lipid metabolism via mitochondrial β-oxidation and microsomal ω-oxidation (Lv et al., 2018). There is a positive correlation between ucOCN and ADPN (El Amrousy and El-Afify, 2020). Vella and Kumar (2013) reported that ucOCN enhanced ADPN release and improved glucose tolerance in mice. Recent research has also demonstrated that activating the ADPN receptors can regulate autophagy in HFD-fed goslings (Cao et al., 2022). The addition of ucOCN significantly alleviated hepatocyte lipid accumulation via the AMPK signaling pathway in oleic acid/palmitic acid treated HepG2 cells (Wang et al., 2023). Furthermore, PPARα and ucOCN can regulate lipid and lipoprotein metabolism and glucose hemostasis (Lv et al., 2018; Tacey et al., 2021). However, there need further study to investigate whether lipophagy play an important role in cellular mechanisms underlying ucOCN effects on the lipid metabolism. Therefore, the aim of this research was to investigate our working hypothesis that ucOCN improves lipophagy in chicken embryonic hepatocytes through activating the ADPN/AMPK and ADPN/PPARα pathways with the potential to reduced FLHS in laying hens (Tu et al., 2023).

In the present study, we used freshly harvested chicken embryonic hepatocytes to investigate the relationship between ucOCN and lipophagy, and to the best of our knowledge, this is the first study to explore the function of ADPN signaling pathway in this progression, promoting the value of ucOCN as a potential protein in regulating the lipid metabolism in FLHS.

MATERIALS AND METHODS

Primary Chicken Embryonic Hepatocytes Isolation and Culture

The isolation and culture of primary chicken hepatocytes was based our previously reported procedure (Zhang et al., 2022b). Ten 15-day-old specific pathogenic free chicken embryos (Shandong Haotai Experimental Animal Breeding Co., Shandong, China) were sterilized and dissected, and the livers were pooled, and cut into small pieces (1 mm × 1 mm), then digested by using 0.25% trypsin-EDTA (Gibco, New York) at 37°C for 30 min. The hepatocytes collected via low-speed centrifugation (1,000 r/min × 5 min), then further purified by centrifugation through 60% Percoll (60% v/v, Biosharp, Anhui, China). Subsequently, primary chicken embryonic hepatocytes at 2×10^5 cells/mL were seeded in 6-well plates with Dulbecco's modified Eagle medium (**DMEM**, Gibco, New York) in a humidified atmosphere containing 95% air and 5% CO_2 at 37°C.

Experimental Design

After the density of hepatocytes reached 80%, they were dividing into 5 groups: control group (CONT, DMEM medium only), FE (Mybiosource, San Diego, CA) treated group (10% FE, v/v), and 3 FE groups plus ucOCN (Mybiosource, San Diego, CA) at 1 ng/mL (FE-LOCN), 3 ng/mL (FE-MOCN), and 9 ng/mL (FE-HOCN) (Zhang et al., 2022b). In the following experiment, to test the effects of ADPN on the function of FE-treated hepatocytes, 4 μM AdipoRon (an adiponectin receptor agonist, MedChemExpress, Shanghai, China) was added with 10% FE in the cell culture fluid. The dose was selected based on the outcomes of our pilot study in which multiple doses (2, 4, 6, 8, and 16 μM) were examined. The cell immunofluorescent staining, real-time PCR analysis, and cell viability were detected after 48 h of treatments, while protein expressions were detected after 72 h of treatments (Zhang et al., 2022b). The culture medium was replaced every 2 d. Six independent cell wells ($n = 6$ per treatment) were used for each of the following examinations

Immunofluorescent Staining

Hepatocytes were fixed by using 4% paraformaldehyde for 20 min and treated with the immunol staining blocking buffer (Beyotime, Shanghai, China) at 4°C for 1 h. LC3 antibody (16/14 kDa; Rabbit Anti-LC3B antibody-N-terminal; 1:1,000; Abcam, Cambridge, United Kingdom) was added to the samples, then the sections were incubated at room temperature for 2 h. Afterward, the sections were stained with a fluorescent secondary antibody (1:500 dilution, goat anti-rabbit antibody; Beyotime, Shanghai, China) and treated with 3.8 μmol/L BODIPY 493/503 (D3922, ThermoFisher Scientific, Waltham, MA), a staining tracer for neutral lipids, for 10 min in the dark (Lee et al., 2014). The nucleus was stained with DAPI (C0065, Solarbio, Beijing, China) through binding to adenine-thymine-rich regions of DNA (Wang et al., 2019). Hepatocytes were visualized via a laser scanning confocal microscope (Leica Microsystems, Wetzlar, Germany) in order to determine the intensity of fluorescence of stained hepatocytes.

Real-Time PCR

The staining procedure was followed the protocol published previously (Wu et al., 2021; Zhang et al., 2022a). Briefly, total RNA was extracted from each hepatocytic sample using Trizol reagent (Invitrogen). The cDNA was synthesized, and Real-time qPCR was performed using SYBR qPCR SuperMix Plus according to the manufacturer's protocol (Novoprotein Scientific Inc., Jiangsu, China). The quantities of mRNA expression of *ADPN, AdipoR1, AdipoR2*, and *PPARα* relative to GAPDH mRNA (glyceraldehyde-3-phosphate dehydrogenase used as a housekeeping gene) were determined using the $2-\Delta\Delta Ct$ method by fluorescent quantitative real-time PCR, where $\Delta Ct = Ct_{\text{target gene}} - Ct_{\text{housekeeping gene}}$. The sequences of primers were designed using the Primer 5.0, synthesized by the Invitrogen Biotechnology (Shanghai, China), and presented in Table 1.

Western Blotting

The total proteins of each hepatocytic sample were extracted using radio-immunoprecipitation assay (**RIPA**) lysate (ThermoFisher, Waltham, MA) with both protease inhibitor and phosphatase inhibitor (Beyotime, Shanghai, China) by following the protocol published previously (Zhang et al., 2022b). Briefly, the proteins were immunolabeled with primary antibodies at 4°C overnight and subsequently incubated with corresponding secondary antibodies at room temperature. The primary antibodies used in this study were: p62 (62 kDa; Rabbit Anti-p62SQSTM1 Polyclonal antibody; 1:3,000; Proteintech, Chicago), Beclin-1 (60 kDa; Rabbit Anti-Beclin-1 antibody; 1:1,000; Cell Signaling, China), LC3 (16/14 kDa; Rabbit Anti-LC3B antibody-N-terminal; 1:1,000; Abcam), AMPK (64 kDa; Rabbit Anti-AMPK alpha 1 antibody; 1:1,000; Bioss, Beijing, China), p-AMPK (64 kDa; Rabbit Anti-phospho-AMPK alpha 2 Ser173+ alpha 1 Ser184 antibody; 1:1,000; Bioss, Beijing, China), ADPN (25 kDa; Rabbit Anti-Adiponectin antibody; 1:1,000; Bioss, Beijing, China), PPARα (51 kDa; Rabbit Anti-PPAR alpha polyclonal antibody; 1:1,000; Bioss, Beijing, China), mTOR (256 kDa; Rabbit Anti-mTOR antibody; 1:1,000; Bioss, Beijing, China), p-mTOR (289 kDa; Rabbit Anti-phospho-mTOR Ser2481; 1:1,000; Bioss, Beijing, China), and GAPDH (36 kDa; mouse anti-GAPDH-loading control antibody; 1:5,000; Bioss, Beijing, China) used as internal control. The secondary antibodies were the HRP-conjugated goat anti-rabbit antibody (1:5,000; ab205718; Beyotime, Shanghai, China) or HRP-conjugated goat anti-mouse antibody (1:5,000; ab205719; Beyotime, Shanghai, China). Finally, SignalFire plus ECL reagent (ThermoFisher, Waltham, MA) was used to show the target bands, then the ImageJ software (version 5.0, BIO-RAD, California) was used to analyze and count the gray value of the bands. GAPDH was used as the internal reference.

Viability Assay and Steatosis

Hepatocytes were assessed for viability using CCK-8 assay kit (Biosharp, Hefei, China) by following the published protocol (Zhang et al., 2022b). Briefly, the cells among all tested concentrations (2, 4, 8, and 16 μM adipoRon) were cultured in 96-well plates for 48 h, and then 10 μL CCK-8 solution was added to incubate for 4 h. After incubation, the optical density (**OD**) values were measured at the 450 nm using a microplate reader (ThermoFisher, Waltham, MA). the Oil red O staining

Table 1. Real-time PCR primers and amplified PCR product size.

Gene	GenBank ID	PCR primers sequence (5′−3′)	PCR products (bp)
PPARα	NM_001001464.1	F: TAGTAAGCTCTCAGAAACTTTGTTG	
		R: AGTCATTTCACTTCACGCAGC	191
Adipo R1	NM_001031027	F: GGAGAAGGTTGTGTTTGGGATGT	
		R: TGGAGAGGTAGATGAGTCTTGGC	218
Adipo R2	NM_001007854	F: ACACACAGAGACTGGCAACATC	
		R: CCCAAGAAGAACAATCCAACAACC	144
ADPN	NM_ 206991.1	F: AAGGAGAGCCAGGTCTACAAGGTG	
		R: GTGCTGCTGTCGTAGTGGTTCTG	238
GAPDH	NM_204305.1	F: TTGACGTGCAGCAGGAACAC	
		R: ATGGCCACCACTTGGACTTT	124

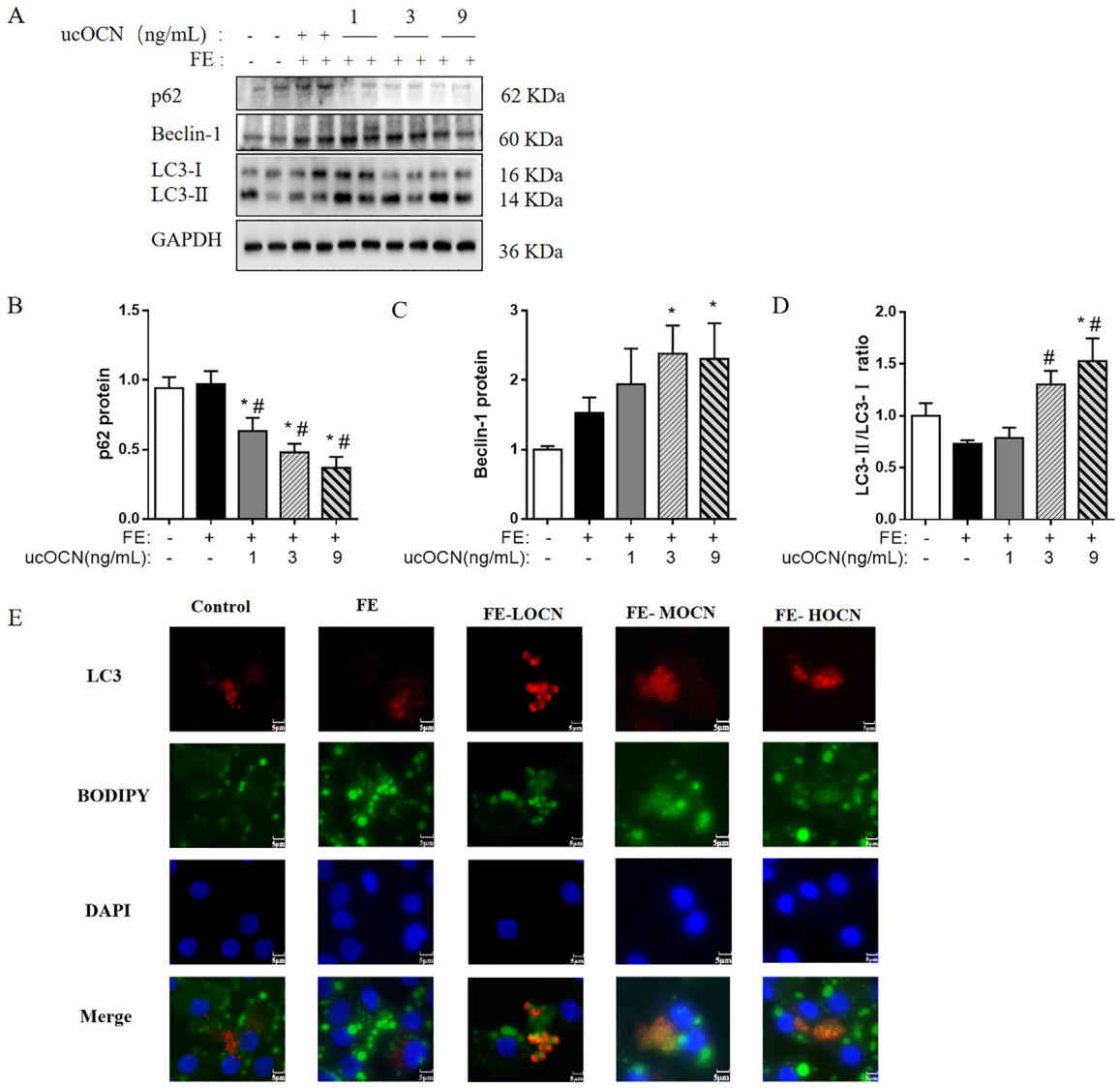

Figure 1. ucOCN activates lipophagy of the FE-induced chicken embryonic hepatocytes. (A) Immunoblot of the autophagy-related protein level of p62, Beclin-1, LC3-Ⅰ, and LC3-Ⅱ; (B) The changes of p62 protein expression; (C) The changes of Beclin-1 protein level; (D) The changes of LC3-Ⅱ/LC3-Ⅱ ratio; (E) The colocalization of LC3 and LDs in the treated chick embryonic hepatocytes. Red: Immunofluorescence of LC3 puncta, Green (BODIPY): Immunofluorescence of LDs, Blue: Immunofluorescence of DAPI. Yellow: The colocalization of LC3 and LDs. The data represent mean ± SEM ($n = 6$ per group). Differences were determined by 1-way ANOVA followed by LSD test. $^*P < 0.05$, compared with the control group, $\#P < 0.05$ compared with the FE group. Abbreviations: Beclin-1, yeast ATG6 homologue; FE, fat emulsion; LC3-Ⅰ, microtubule-associated proteins light chain 3-Ⅰ; LC3-Ⅱ, microtubule-associated proteins light chain 3-Ⅱ; P62, P62/SQSTM1; ucOCN, undercarboxylated osteocalcin.

(Nanjing Jiancheng Bioengineering Institute, Nanjing, China) for light microscopic examinations and quantitative analysis according to the assay kit manufacturer's instructions. TG content analysis was performed to examine the lipid accumulation in the hepatocytes according to the protocols provided by the manufacturer (Nanjing Jiancheng Bioengineering Institute, Nanjing, China).

Statistical Analyses

Data were analyzed using SPSS 22.0 (IBM Co., New York, NY). One-way ANOVA was used to analyze the differences among the groups and data normality was checked. Post hoc multiple comparisons were performed using LSD's test. Values were expressed as mean ± SEM, and $P < 0.05$ was defined statistically significant.

RESULTS

ucOCN Activates Lipophagy in the FE-Induced Chicken Embryonic Hepatocytes

Western-blotting bands are shown in Figure 1A. The data analysis indicated that compared with CONT and FE groups, ucOCN treatment resulted in a dose-dependent reduction of p62 ($P < 0.05$, Figure 1B), a protein involved in autophagic degradation. Compared with CONT group, 3 and 9 ug/mL ucOCN significantly increased Beclin-1, an autophagy biomarker ($P < 0.05$, Figure 1C), while 9 ug/mL ucOCN raised LC3-II/LC3-I

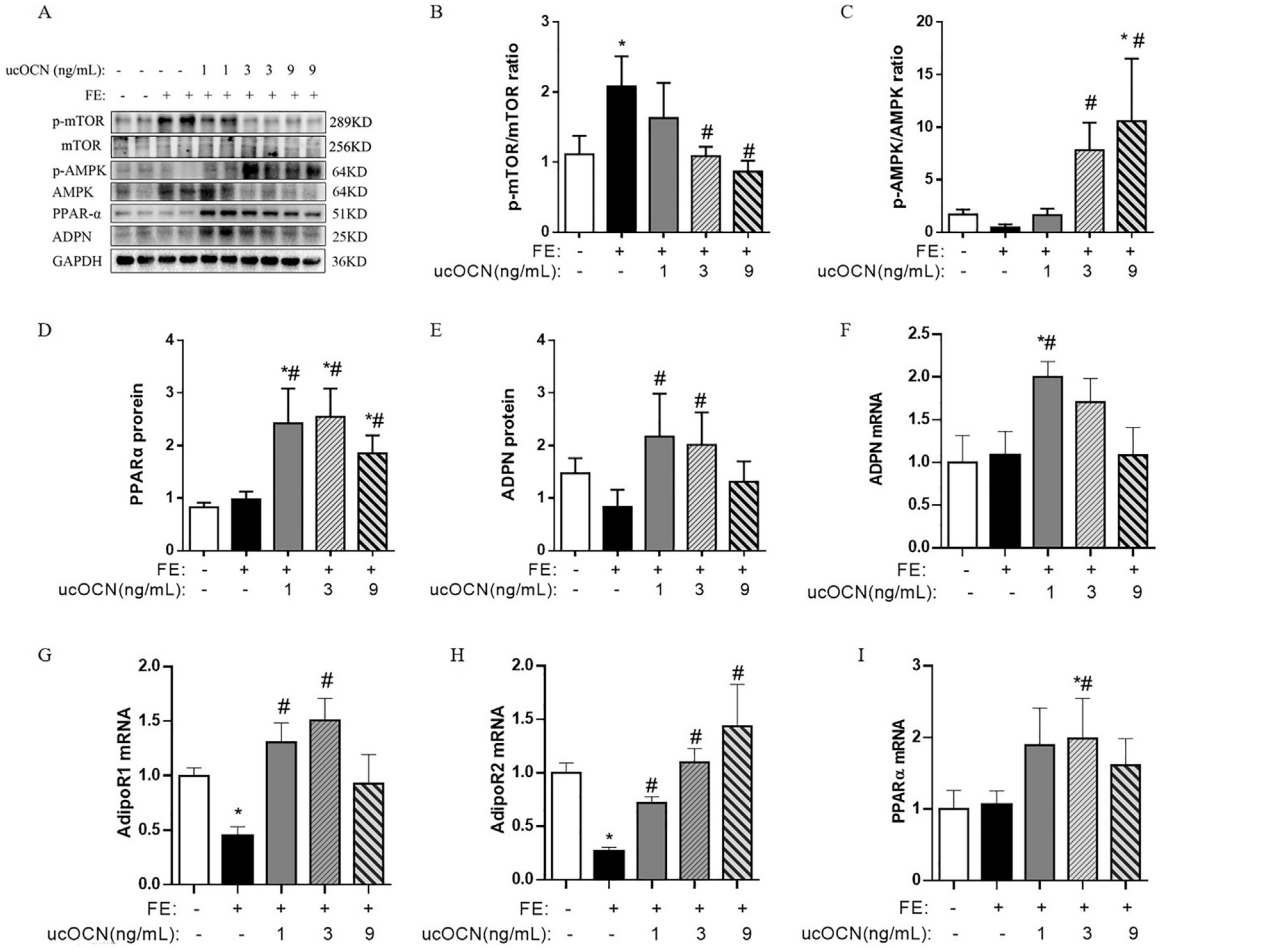

Figure 2. ucOCN activates the ADPN-AMPK/PPARα-mTOR signaling pathway in the treated chicken embryonic hepatocytes. (A) Immunoblot of p-mTOR, mTOR, p-AMPK, AMPK, PPARα and ADPN protein; (B) The changes of p-mTOR/mTOR ratio; (C) The changes of p-AMPK/AMPK ratio; (D) The changes of PPARα protein level; (E) The changes of ADPN protein level; (F) The changes of ADPN mRNA expressions; (G) The changes of AdipoR1 mRNA expressions; (H) The changes of AdipoR2 mRNA expressions; (I) The changes of PPARα mRNA expressions. The data represent mean ± SEM ($n = 6$ per group). Differences were determined by 1-way ANOVA followed by LSD test. *$P < 0.05$ compared with the control group, #$P < 0.05$ compared with the FE group. Abbreviations: AdipoR1, adiponectin receptor 1; AdipoR2, adiponectin receptor 2; ADPN, adiponectin; AMPK, adenosine 5′-monophosphate (AMP)-activated protein kinase; FE, fat emulsion; mTOR, the mammalian target of rapamycin; PPARα, peroxisome proliferators-activated receptor α; ucOCN, undercarboxylated osteocalcin.

ratio ($P < 0.05$, Figure 1D) in hepatocytes. Furthermore, compared with FE group, the cells of both FE-MOCN and FE-HOCN groups had a higher LC3-II/LC3-I ratio ($P < 0.05$).

The colocalization analysis of the LC3 and the LDs in hepatocytes was conducted using double staining, LC3 (red) and Bodipy 493/503 (green) and presents in Figure 1E. The results indicated that lipophagy was induced in the hepatocytes, evidenced by the presence of cells with yellow color in ucOCN treated cells. All the above results indicated that ucOCN induces lipophagy in FE-treated hepatocytes.

ucOCN Activates the ADPN-AMPK/PPARα-mTOR Signaling Pathway in the FE-Induced Chicken Embryonic Hepatocytes

The treatment induced changes of protein expressions of the parameters involving in the ADPN-AMPK/PPARα-mTOR signaling pathway are presented in Figure 2. Compared to the CONT embryonic hepatocytes, FE increased the ratio of p-mTOR/mTOR in the embryonic hepatocytes, while the effects of FE were suppressed by ucOCN at both 3 and 9 ng/mL ($P < 0.05$, Figure 2A, B). In addition, the ratio of p-AMPK/AMPK in the hepatocytes was increased in both FE-MOCN and FE-HOCN groups compared to FE group, especially in FE-HOCN group which was higher than both CONT and FE groups ($P < 0.05$, Figure 2 C). All tested ucOCN dosages significantly increased the hepatocyte PPARα levels compared to both CONT and FE groups ($P < 0.05$, Figure 2D). In addition, ADPN proteins level of the hepatocytes showed increase in 1 and 3 ng/mL ucOCN concentrations compared to FE group but not CONT group ($P < 0.05$, Figure 2E).

Compared with CONT and FE group, 1 ng/mL ucOCN increased the *ADPN* mRNA expression in chicken embryonic hepatocytes ($P < 0.05$, Figure 2F). Compared with control group, FE decreased both *AdipoR1* and *AdipoR2* mRNA expressions ($P < 0.05$, Figure 2G, H), while ucOCN at 1 and 3 ng/mL upregulated the *AdipoR1* mRNA expression ($P < 0.05$) and ucOCN at all tested concentrations increased the

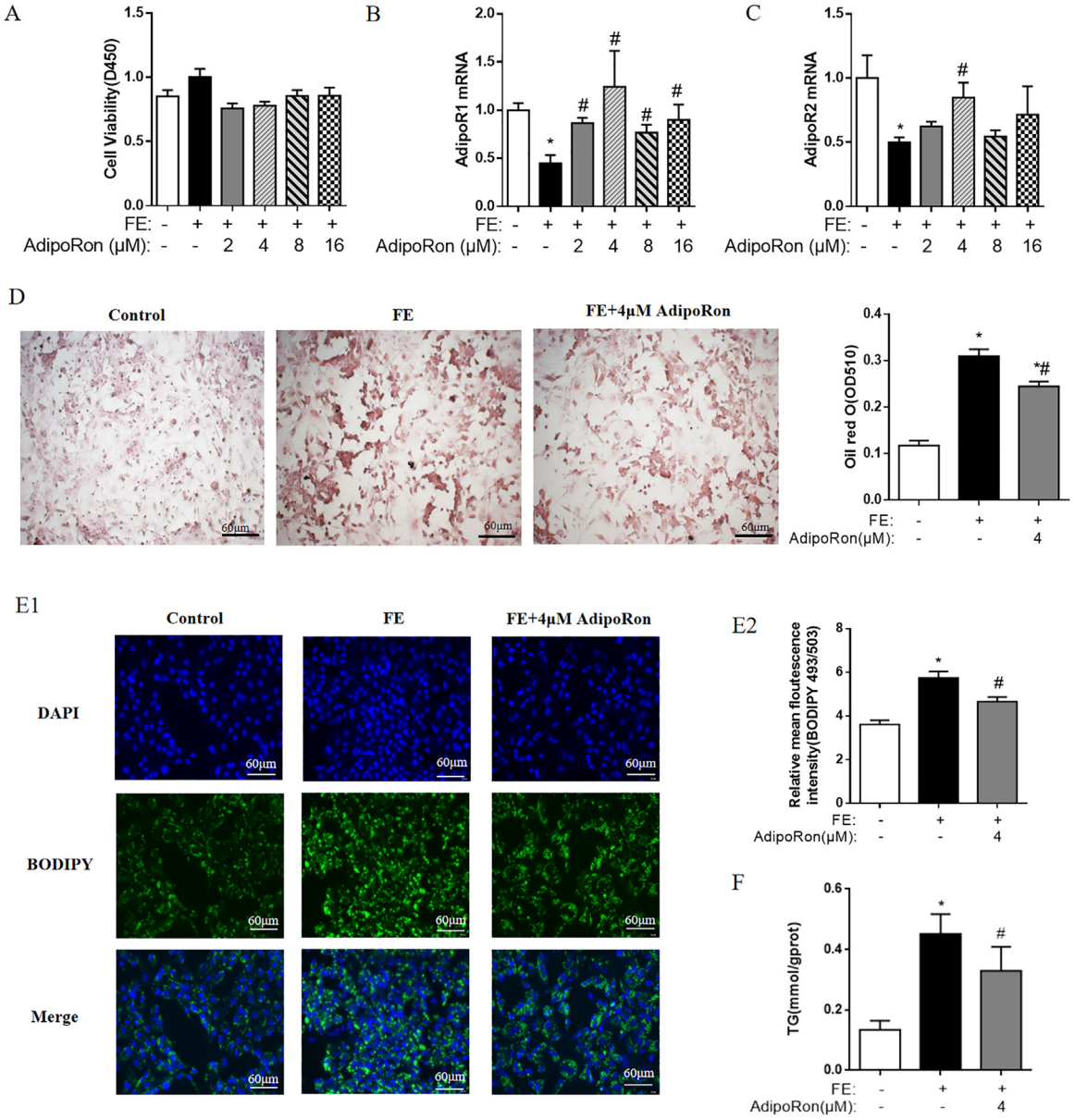

Figure 3. AdipoRon ameliorates fat accumulation in the FE-induced chicken embryonic hepatocytes. (A) The cell viability; (B) The changes of AdipoR1 mRNA expressions; (C) The changes of AdipoR2 mRNA expressions; (D) The levels of intracellular lipid droplets indicated by the Oil red staining and quantitative analysis of Oil red O; (E) Immunofluorescence of BODIPY (LDs); (F) The change of TG concentration. The data represent mean ± SEM ($n = 6$ per group). Differences were determined by 1-way ANOVA followed by LSD test. $^*P < 0.05$ compared with control group, $\#P < 0.05$ compared with FE group. Abbreviations: AdipoRon, adiponectin receptor agonists; AdipoR1, adiponectin receptor 1; AdipoR2, adiponectin receptor 2; FE, fat emulsion; ucOCN, undercarboxylated osteocalcin.

AdipoR2 mRNA expression with a dosage-depended pattern ($P < 0.05$). For the mRNA expression level of *PPARα*, 3 ng/mL ucOCN increased its expression ($P < 0.05$, Figure 2I) compared to both CONT and FE groups.

AdipoRon Ameliorates Fat Accumulation in the Treated Chicken Embryonic Hepatocytes

To further understand the role of the ADPN signaling pathway in autophagy, different concentrations of AdipoRon were added with or without FE. CCK-8 analysis showed that there were no treatment effects on cell viability ($P > 0.05$, Figure 3A). The qPCR results indicated that FE decreased the *AdipoR1* and *AdipoR2* mRNA expression ($P < 0.05$, Figure 3B, C) in embryonic hepatocytes, while *AdipoR1* and *AdipoR2* mRNA expression was improved mostly after treated with 4 μM AdipoRon among all the tested concentrations ($P < 0.05$). Therefore, 4 μm AdipoRon was used for further experiments.

Oil red O staining showed that the addition of FE dramatically increased the intracellular lipid droplets in hepatocytes, the effects was alleviated by administrated AdipoRon but the levels of intracellular lipid droplets were still higher than that of CONT group ($P < 0.05$, Figure 3D). Similarly, BODIPY staining showed an increase in fluorescence intensity following FE treatment, which was diminished with AdipoRon treatment ($P < 0.05$, Figure 3E1, E2). Cellular TG content analysis

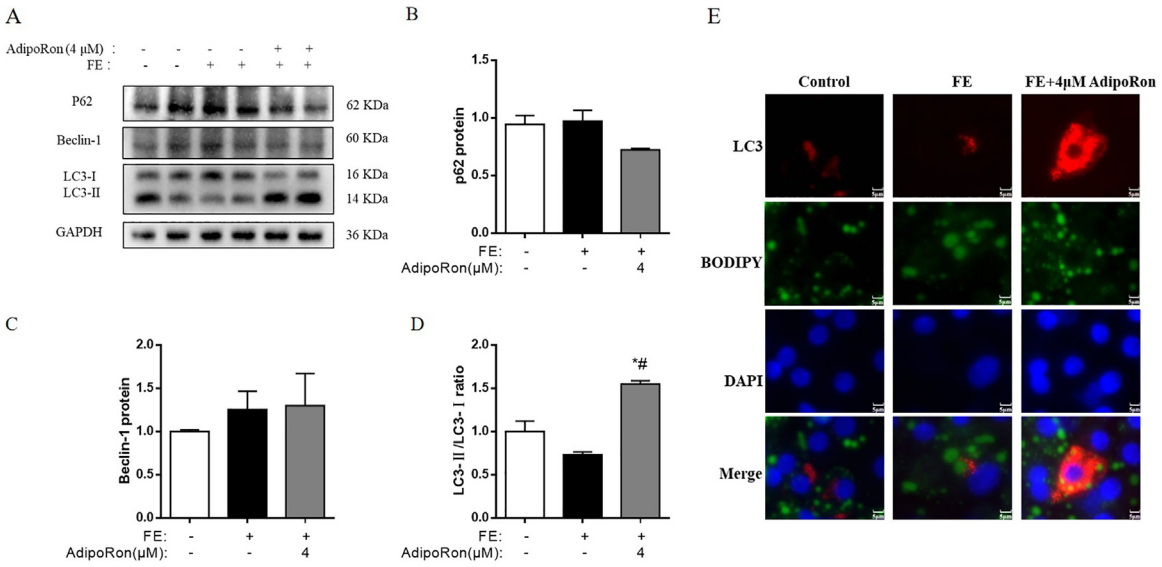

Figure 4. AdipoRon activates lipophagy in the FE-induced chicken embryonic hepatocytes. (A) Immunoblot of the autophagy-related protein level of p62, Beclin-1, LC3-Ⅰ, and LC3-Ⅱ; (B) The change of p62 protein expression; (C) The change of Beclin-1 protein level; (D) The change of LC3-Ⅱ/LC3-Ⅰ ratio; (E) The colocalization of LC3 and LDs in FE-induced chick embryo hepatocytes. Red: Immunofluorescence of LC3 puncta, Green (BODIPY): Immunofluorescence of LDs, Blue: Immunofluorescence of DAPI. Merge showed the colocalization of LC3 and LDs. The data represent mean ± SEM ($n = 6$ per group). Differences were determined by 1-way ANOVA followed by LSD test. $^*P < 0.05$, compared with the control group, $\#P < 0.05$ compared with the FE group. Abbreviations: Beclin-1, yeast ATG6 homologue; FE, fat emulsion; LC3-Ⅰ, microtubule-associated proteins light chain 3-Ⅰ; LC3-Ⅱ, microtubule-associated proteins light chain 3-Ⅱ; P62, P62/SQSTM1; ucOCN, undercarboxylated osteocalcin.

showed that compared to the controls, FE significantly increased fat accumulation in the chicken embryonic hepatocytes, evidenced by increased TG concentrations, and this change was significantly reduced by adding 4 μM AdipoRon (Figure 3F).

AdipoRon Activates Lipophagy in the FE-Induced Chicken Embryonic via Activating the AMPK/PPARA-mTOR Signaling Pathway

The changes of autophagy proteins expressions (p62, Beclin-1, LC3-II, and LC3-I) are shown in Figure 4A. Compared to hepatocytes of CONT group, FE did not affect the concentrations of p62 ($P > 0.05$, Figure 4B), Becllin-1 ($P > 0.05$, Figure 4C), and LC3-II/LC3-I ratios ($P > 0.05$, Figure 4D). However, AdipoRon resulted in higher LC3-II/LC3-I ratios in AdipoRon group than both CONT and FE groups (Figure 4D). The immunofluorescence results showed AdipoRon induced the colocalization of LC3 and LDs in fatty hepatocytes (Figure 4E).

Moreover, compared with the control group, p-mTOR protein expression was increased in the FE group leading to a higher p-mTOR/mTOR ratio ($P < 0.05$, Figure 5A, B). However, these effects of FE were decreased upon AdipoRon treatment. Additionally, AdipoRon activated the p-AMPK/AMPK ratio ($P < 0.05$, Figure 5C) and protein expression of PPARα ($P < 0.05$, Figure 5D) than that of CONT and FE groups.

DISCUSSION

Nutrition is the most vital factor for hens to maintain high production, while overdosing on energy is the major cause of hen's FLHS (Choi et al., 2012; Meng et al., 2021). Research showed that one of the characteristics of experimental hen's FLHS is obese with great accumulating fatty acid, TG, and LDs in hepatocytes (Rozenboim et al., 2016; Shini et al., 2020; Lin et al., 2021; Miao et al., 2021). FE-induced high level of TG and mass of LDs in hepatocytes has been used as a successful liver steatosis cell model (Zhang et al., 2022a, b). In our previous studies, we reported that 1, 3, and 9 ng/mL ucOCN markedly reduced LDs quantity and TG concentrations, alleviated fat accumulation in FE stimulated chicken embryonic hepatocytes (Zhang et al., 2022b). And HFD inhibited autophagy in laying hens by strikingly declined the mRNA levels of Beclin-1, Atg5, and Atg7, resulting from excessive fat deposition (Wang et al., 2020b; Wu et al., 2021). The current study further revealed that ucOCN regulates lipid metabolism in chicken embryonic hepatocytes by enhancing lipophagy via the ADPN-AMPK/PPARα-mTOR signaling pathway.

The autophagic level was reduced in FE treated hepatocytes via downregulated LC3-II expression, reflecting the inhibition of autophagy in chicken liver steatosis (Du et al., 2023). Autophagic activation breaks down undesirable lipids via increasing lipid metabolism (Lamark and Johansen, 2012). Intermittent administration of ucOCN (i.p. injection once a day for 8 wk) reverses the attenuated autophagy in obese mice, decreasing body and fat-pad weight gain, and serum triglycerides (Zhou et al., 2016). Our previous study demonstrated that ucOCN activated hepatocyte autophagy and prevented insulin resistance and hepatic inflammation in HFD-induced FLHS chickens (Wu et al., 2021). LC3-II is a biological marker for autophagosome-lysosomal turnover (Tanida et al., 2008). The binding LC3-II to the cellular

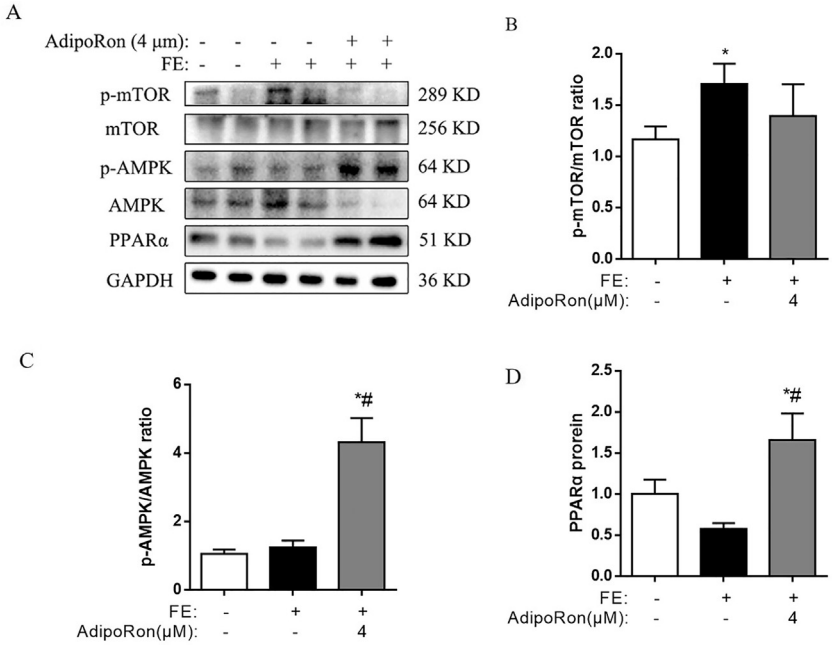

Figure 5. Effects of AdipoRon on AMPK/PPARα-mTOR signaling pathway in chicken embryonic hepatocytes. (A) Immunoblot of p-mTOR, mTOR, p-AMPK, AMPK, PPARα protein; (B) The change of p-mTOR/mTOR ratio; (C) The change of p-AMPK/AMPK ratio; (D) The change of PPAR α protein level. The data represent mean ± SEM ($n = 6$ per group). Differences were determined by 1-way ANOVA followed by LSD test. $^*P < 0.05$ compared with the control group, $\#P < 0.05$ compared with the CONT or FE group. Abbreviations: AdipoRon, adiponectin receptor agonists; AMPK, adenosine 5′-monophosphate (AMP)-activated protein kinase; FE, fat emulsion; mTOR, the mammalian target of rapamycin; PPARα, peroxisome proliferators-activated receptor α; ucOCN, undercarboxylated osteocalcin.

membrane is an important biological process of autophagy, and the further formation of autophagic membrane is accompanied by the increase of LC3-II (Xu and Wan, 2023). Soluble LC3-I is converted into LC3-II (membrane-bound LC3-phosphatidylethanolamine), as the initial step of autophagy, and the autophagy capability can be determined by LC3-II/LC3-I ratio (Xu and Wan, 2023). During the autophagic circling, SQSTM1/p62, as an adaptor protein of selective autophagy, is requested for the macroautophagic process, promoting autophagy activation for lipid metabolism (Xu and Wan, 2023). In this study, the results showed that 3 and 9 ng/mL ucOCN added to FE-treated hepatocytes increased autophagy activity by upregulating the levels of Beclin-1, and LC3-II/LC3-I ratio, while downregulated p62. Those results indicate that ucOCN functionally regulates LC3 metabolism.

Lipid droplet, as a cellular organelle, plays a critical role in lipid metabolisms, maintaining cellular energy balance (Jin et al., 2023). Elevated amount of LDs is a hallmark of nonalcoholic fatty liver disease (**NAFLD**) in humans (Scorletti and Carr, 2022) and FLHS in chickens (You et al., 2023). Lipophagy is a novel approach to reduce hepatic disorders via regulating lipid metabolism (Singh et al., 2009), and the colocalization of LDs and LC3 is a direct biological marker between LDs and autophagosomes (Singh et al., 2009). Induction of autophagy by rapamycin (an autophagy activator) increases LDs and LC3 colocalization in untreated and oleate-treated cells (Singh et al., 2009). In this study, the colocalization of LC3 and LDs in ucOCN-treated hepatocytes indicated ucOCN is involved in lipophagy activation. Therefore, ucOCN can promote lipophagy in FE-induced primary chicken hepatocytes. The results may provide new insights for controlling FLHS in laying hens.

A few results have proposed that the positive correlation between ucOCN and ADPN in humans (El Amrousy and El-Afify, 2020), however, it has not been clarified in chickens. ADPN is well known for decreasing gluconeogenesis by stimulating glycolysis and fatty acid oxidation and improving insulin sensitivity in the liver (Gamberi et al., 2018). Administration of ADPN restores the ethanol-induced accumulation of p62, a marker of autophagy flux in liver cells (Nepal et al., 2014). Activation of ADPN receptors also has a protective effect on fatty liver injury in HFD-fed goslings through its downstream pathways, the AMPK and PPARα signaling pathways, regulating autophagy (Cao et al., 2022). AMPK is one of the most well-recognized modulators of the guardians of lipid homeostasis and is suppressed in FLHS, regulating AMPK metabolism has been considered as a promising therapeutic target for FLHS (Yao et al., 2022a, b). PPARα is a regulator of lipid and lipoprotein metabolism and glucose homeostasis, and PPARα activation can promote autophagy and reduce hepatic fat accumulation (Yoo et al., 2021). The current study showed that ucOCN activated the genes and protein expressions of ADPN and AdipoR, AMPK, and PPARα in the liver, suggesting that ucOCN activates ADPN-AMPK/ PPARα signaling pathway in FE-induced chicken hepatocytes.

Mechanistic target of rapamycin (**mTOR**), a highly conserved serine/threonine-protein kinase that belongs to the phosphoinositide 3 kinase-related kinase family, plays a pivotal role in autophagy regulation (Khawar et

al., 2019), and AMPK-mTOR axis is a key pathway for autophagy in chickens (Liao et al., 2020; Li et al., 2021). Upregulation of the AMPK/mTOR signaling pathway activates autophagy to mitigate hepatic steatosis via promoting fatty acid oxidation (Zhang et al., 2020). ADPN promotes autophagy via suppressed mTOR phosphorylation in mice, which is eliminated by compound C (AMPK inhibitor) (Hu et al., 2017). In the current study, FE promoted mTOR phosphorylation and inhibited autophagy, while 3 ng/mL ucOCN increased ADPN and PPARα protein levels, and p-AMPK/AMPK ratio and decreased p-mTOR protein expression, indicating that ucOCN activates ADPN- AMPK/PPARα-mTOR signaling pathway.

To further gain insights into the ucOCN stimulating the signaling pathways in lipophagy, AdipoRon, an ADPN receptor agonist, was used in this study for investigating the function of ADPN signaling pathway in autophagy. Wang et al. (2020a) demonstrated that AdipoRon upregulated LC3-II/LC3-I ratio, downregulated p62 protein expression in myeloma cells via the AMPK pathway. Cao et al. (2022) illustrated that AdipoRon can alter the expression of autophagy-related genes beclin-1 and LC3. Similarly, our results demonstrated that AdipoRon had a wide safety margin and 4 μM was the optimal concentration of AdipoRon for activating its receptors. Similar to the functions of ucOCN, AdipoRon attenuates fat accumulation, prevents lipid metabolic disorders in hepatocytes (Zhang et al., 2022b). The increased LC3-II protein expression further implied that AdipoRon promotes autophagy activation. The LC3 and LDs colocalization observed by immunofluorescence in AdipoRon treated group revealed lipophagy in FE-induced hepatocytes. Furthermore, AdipoRon activated the AMPK/PPARα-mTOR signaling pathway to regulate lipid metabolism. Taken together, ucOCN ameliorates fat accumulation and activates autophagy via the ADPN-AMPK/PPARα-mTOR signaling pathway.

CONCLUSIONS

The results of this study further reveal that fat emulsion inhibits the autophagy in primary chicken embryonic hepatocytes. ucOCN has functions in regulating lipid metabolism in hepatocytes. Especially, ucOCN activates lipophagy via the ADPN- AMPK/PPARα-mTOR signaling pathway. The results may provide new insights for controlling FLHS in laying hens.

ACKNOWLEDGMENTS

This research was supported by the National Natural Science Foundation of China (No. 31702307); Chongqing Graduate Scientific Research Innovation Project (CYS23234); Fundamental Research Funds for the Central Universities (SWU-XDJH202307); Chongqing Municipal Training Program of Innovation and Entrepreneurship for Undergraduates（S202210635023).

DISCLOSURES

There is no conflict of interest to declare.

REFERENCES

Bessone, F., M. V. Razori, and M. G. Roma. 2019. Molecular pathways of nonalcoholic fatty liver disease development and progression. Cell. Mol. Life Sci. 76:99–128.

Cao, Z., B. Ma, C. Cui, J. Zhao, S. Liu, Y. Qiu, Y. Zheng, M. Gao, and X. Luan. 2022. Protective effects of AdipoRon on the liver of Huoyan goose fed a high-fat diet. Poult. Sci. 101:101708.

Choi, Y. I., H. J. Ahn, B. K. Lee, S. T. Oh, B. K. An, and C. W. Kang. 2012. Nutritional and hormonal induction of fatty liver syndrome and effects of dietary lipotropic factors in egg-type male chicks. Asian-Australas. J. Anim. Sci. 25:1145–1152.

Du, Z. Q., Y. Q. Pang, Y. Zhang, L. Wang, R. Zhang, H. Li, and C. X. Yang. 2023. Folate inhibits lipid deposition via the autophagy pathway in chicken hepatocytes. Poult. Sci. 102:102363.

El Amrousy, D., and D. El-Afify. 2020. Osteocalcin and osteoprotegerin levels and their relationship with adipokines and proinflammatory cytokines in children with nonalcoholic fatty liver disease. Cytokine 135:155215.

Gamberi, T., F. Magherini, A. Modesti, and T. Fiaschi. 2018. Adiponectin signaling pathways in liver diseases. Biomedicines 6:52.

Hu, J. Z., W. D. Cui, W. X. Ding, Y. Q. Gu, Z. Wang, and W. M. Fan. 2017. Globular adiponectin attenuated H_2O_2-induced apoptosis in rat chondrocytes by inducing autophagy through the AMPK/mTOR pathway. Cell. Physiol. Biochem. 43:367–382.

Jin, Y., Y. Tan, J. Wu, and Z. Ren. 2023. Lipid droplets: a cellular organelle vital in cancer cells. Cell Death Discov. 9:254.

Khawar, M. B., H. Gao, and W. Li. 2019. Autophagy and lipid metabolism. Autophagy: Biology and Diseases, Springer, Singapore 359–374.

Lamark, T., and T. Johansen. 2012. Aggrephagy: selective disposal of protein aggregates by macroautophagy. Int. J. Cell Biol. 2012:736905.

Lee, J. M., M. Wagner, R. Xiao, K. H. Kim, D. Feng, M. A. Lazar, and D. D. Moore. 2014. Nutrient-sensing nuclear receptors coordinate autophagy. Nature 516:112–115.

Li, Z., Z. Miao, L. Ding, X. Teng, and J. Bao. 2021. Energy metabolism disorder mediated ammonia gas-induced autophagy via AMPK/mTOR/ULK1-Beclin1 pathway in chicken livers. Ecotoxicol. Environ. Saf. 217:112219.

Liao, J., F. Yang, W. Yu, N. Qiao, H. Zhang, Q. Han, L. Hu, Y. Li, J. Guo, J. Pan, and Z. Tang. 2020. Copper induces energy metabolic dysfunction and AMPK-mTOR pathway-mediated autophagy in kidney of broiler chickens. Ecotoxicol. Environ. Saf 206:111366.

Lin, C. W., T. W. Huang, Y. J. Peng, Y. Y. Lin, H. J. Mersmann, and S. T. Ding. 2021. A novel chicken model of fatty liver disease induced by high cholesterol and low choline diets. Poult. Sci. 100:100869.

Lv, Z., K. Xing, G. Li, D. Liu, and Y. Guo. 2018. Dietary genistein alleviates lipid metabolism disorder and inflammatory response in laying hens with fatty liver syndrome. Front. Physiol. 9:1493.

Meng, J., N. Ma, H. Liu, J. Liu, J. Liu, J. Wang, X. He, and X. Zhao. 2021. Untargeted and targeted metabolomics profiling reveals the underlying pathogenesis and abnormal arachidonic acid metabolism in laying hens with fatty liver hemorrhagic syndrome. Poult. Sci. 100:101320.

Miao, Y. F., X. N. Gao, D. N. Xu, M. C. Li, Z. S. Gao, Z. H. Tang, N. H. Mhlambi, W. J. Wang, W. T. Fan, X. Z. Shi, G. L. Liu, and S. Q. Song. 2021. Protective effect of the new prepared Atractylodes macrocephala Koidz polysaccharide on fatty liver hemorrhagic syndrome in laying hens. Poult. Sci. 100:938–948.

Nepal, S., M. J. Kim, E. S. Lee, J. A. Kim, D. Y. Choi, D. H. Sohn, S. H. Lee, K. Song, S. H. Kim, G. S. Jeong, T. C. Jeong, and P. H. Park. 2014. Modulation of Atg5 expression by globular adiponectin contributes to autophagy flux and suppression of ethanol-induced cell death in liver cells. Food Chem. Toxicol. 68:11–22.

Rozenboim, I., J. Mahato, N. A. Cohen, and O. Tirosh. 2016. Low protein and high-energy diet: a possible natural cause of fatty liver hemorrhagic syndrome in caged White Leghorn laying hens. Poult. Sci. 95:612–621.

Scorletti, E., and R. M. Carr. 2022. A new perspective on NAFLD: focusing on lipid droplets. J. Hepatol. 76:934–945.
Shini, S., A. Shini, and W. L. Bryden. 2020. Unravelling fatty liver haemorrhagic syndrome: 1. Oestrogen and inflammation. Avian Pathol. 49:87–98.
Shini, A., S. Shini, and W. l. Bryden. 2018. Fatty liver haemorrhagic syndrome occurrence in laying hens: impact of production system. Avian Pathol. 48:1–32.
Singh, R., S. Kaushik, Y. Wang, Y. Xiang, I. Novak, M. Komatsu, K. Tanaka, A. M. Cuervo, and M. J. Czaja. 2009. Autophagy regulates lipid metabolism. Nature 458:1131–1135.
Tacey, A., A. Hayes, A. Zulli, and I. Levinger. 2021. Osteocalcin and vascular function: is there a cross-talk? Mol. Metab. 49:101205.
Tanida, I., T. Ueno, and E. Kominami. 2008. LC3 and autophagy. Methods Mol. Biol. 445:77–88.
Tu, W., Y. Zhang, K. Jiang, and S. Jiang. 2023. Osteocalcin and its potential functions for preventing fatty liver hemorrhagic syndrome in poultry. Animals 13:1380.
Vella, A., and R. Kumar. 2013. Osteocalcin and the regulation of glucose metabolism. Clin. Rev. Bone Miner Metab. 11:11–16.
Wang, G., Z. Man, N. Zhang, H. Xin, Y. Li, T. Sun, and S. Sun. 2019. Biopanning of mouse bone marrow mesenchymal stem cell affinity for cyclic peptides. Mol. Med. Rep. 19:407–413.
Wang, S. J., C. Wang, W. Q. Wang, Q. Q. Hao, and Y. F. Liu. 2020a. Adiponectin receptor agonist AdipoRon inhibits the proliferation of myeloma cells via the AMPK/autophagy pathway. Zhongguo Shi Yan Xue Ye Xue Za Zhi 28:171–176.
Wang, X., C. Xing, F. Yang, S. Zhou, G. Li, C. Zhang, H. Cao, and G. Hu. 2020b. Abnormal expression of liver autophagy and apoptosis-related mRNA in fatty liver haemorrhagic syndrome and improvement function of resveratrol in laying hens. Avian Pathol. 49:171–178.
Wang, D., M. Zhang, J. Xu, and J. Yang. 2023. Uncarboxylated osteocalcin decreases SCD1 by activating AMPK to alleviate hepatocyte lipid accumulation. Molecules 28:3121.
Wu, X. L., X. Y. Zou, M. Zhang, H. Q. Hu, X. L. Wei, M. L. Jin, H. W. Cheng, and S. Jiang. 2021. Osteocalcin prevents insulin resistance, hepatic inflammation, and activates autophagy associated with high-fat diet-induced fatty liver hemorrhagic syndrome in aged laying hens. Poult. Sci. 100:73–83.
Xu, C., and J. Fan. 2022. Links between autophagy and lipid droplet dynamics. J. Exp. Bot. 73:2848–2858.
Xu, Y., and W. Wan. 2023. Acetylation in the regulation of autophagy. Autophagy 19:379–387.
Yao, Y., L. Li, H. Wang, Y. Yang, and H. Ma. 2022a. Activated AMP-activated protein kinase prevents hepatic steatosis, oxidative stress and inflammation in primary chicken hepatocytes. Front. Physiol. 13:974825.
Yao, Y., H. Wang, Y. Yang, Z. Jiang, and H. Ma. 2022b. Dehydroepiandrosterone activates the GPER-mediated AMPK signaling pathway to alleviate the oxidative stress and inflammatory response in laying hens fed with high-energy and low-protein diets. Life Sci. 308:120926.
Yoo, J., I. K. Jeong, K. J. Ahn, H. Y. Chung, and Y. C. Hwang. 2021. Fenofibrate, a PPARα agonist, reduces hepatic fat accumulation through the upregulation of TFEB-mediated lipophagy. Metabolism 120:154798.
You, M., S. Zhang, Y. Shen, X. Zhao, L. Chen, J. Liu, and N. Ma. 2023. Quantitative lipidomics reveals lipid perturbation in the liver of fatty liver hemorrhagic syndrome in laying hens. Poult. Sci. 102:102352.
Zhang, J., H. Du, M. Shen, Z. Zhao, and X. Ye. 2020. Kangtaizhi granule alleviated nonalcoholic fatty liver disease in high-fat diet-fed rats and HepG2 cells via AMPK/mTOR signaling pathway. J. Immunol. Res. 2020:3413186.
Zhang, C., S. Meng, C. Li, Z. Yang, G. Wang, X. Wang, and Y. Ma. 2022a. Primary broiler hepatocytes for establishment of a Steatosis model. Vet. Sci. 9:316.
Zhang, M., W. J. Tu, Q. Zhang, X. L. Wu, X. Y. Zou, and S. Jiang. 2022b. Osteocalcin reduces fat accumulation and inflammatory reaction by inhibiting ROS-JNK signal pathway in chicken embryonic hepatocytes. Poult. Sci. 101:102026.
Zhou, B., H. Li, J. Liu, L. Xu, Q. Guo, W. Zang, H. Sun, and S. Wu. 2016. Autophagic dysfunction is improved by intermittent administration of osteocalcin in obese mice. Int. J. Obes. (Lond.) 40:833–843.
Zhuang, Y., C. Xing, H. Cao, C. Zhang, J. Luo, X. Guo, and G. Hu. 2019. Insulin resistance and metabonomics analysis of fatty liver haemorrhagic syndrome in laying hens induced by a high-energy low-protein diet. Sci. Rep. 9:10141.